

**ICEF2020-20147**

**CONTROLLED END GAS AUTO IGNITION WITH EXHAUST GAS RECIRCULATION ON A  
STOICHIOMETRIC, SPARK IGNITED, NATURAL GAS ENGINE**

**Scott Bayliff**

Colorado State University  
Department of Mechanical Engineering  
Fort Collins, CO, USA

**Bret Windom**

Colorado State University  
Department of Mechanical Engineering  
Fort Collins, CO, USA

**Anthony Marchese**

Colorado State University  
Department of Mechanical Engineering  
Fort Collins, CO, USA

**Greg Hampson**

Woodward Inc.  
Fort Collins, CO, USA

**Jeffrey Carlson**

Woodward Inc.  
Fort Collins, CO, USA

**Domenico Chiera**

Woodward Inc.  
Fort Collins, CO, USA

**Daniel Olsen**

Colorado State University  
Department of Mechanical Engineering;  
Fort Collins, CO, USA

**ABSTRACT**

The goal of this study is to address fundamental limitations to achieving diesel-like efficiencies in heavy duty on-highway natural gas (NG) engines. Engine knock and misfire are barriers to pathways leading to higher efficiency engines. This study explores enabling technologies for development of high efficiency stoichiometric, spark ignited, natural gas engines. These include design strategies for fast and stable combustion and higher dilution tolerance. Additionally, advanced control methodologies are implemented to maintain stable operation between knock and misfire limits. To implement controlled end-gas autoignition (C-EGAI) strategies a Combustion Intensity Metric (CIM) is used for ignition control with the use of a Woodward large engine control module (LECM).

Tests were conducted using a single cylinder, variable compression ratio, cooperative fuel research (CFR) engine with baseline conditions of 900 RPM, engine load of 800 kPa indicated mean effective pressure (IMEP), and stoichiometric air/fuel ratio. Exhaust gas recirculation (EGR) tests were performed using a custom EGR system that simulates a high pressure EGR loop and can provide a range of EGR rates from 0 to 40%. The experimental measurements included the variance of EGR rate, compression ratio, engine speed, IMEP, and CIM. These five variables were optimized through a Modified Box-Benken design Surface Response Method (RSM), with brake efficiency as the merit function.

A positive linear correlation between CIM and f-EGAI was identified. Consequently, CIM was used as the feedback control parameter for C-EGAI. As such, implementation of C-EGAI effectively allowed for the utilization of high EGR rates and CRs, controlling combustion between a narrower gap between knock and lean limits. The change from fixed to parametric ignition timing with CIM targeted select values of f-EGAI with an average coefficient of variance (COV) of peak pressure of 5.4. The RSM efficiency optimization concluded with operational conditions of 1080 RPM, 1150 kPa IMEP, 10.55:1 compression ratio, and 17.8% EGR rate with a brake efficiency of 21.3%. At this optimized point of peak performance, a f-EGAI for C-EGAI was observed at 34.1% heat release due to auto ignition, a knock onset crank angle value of 10.3° aTDC and ignition timing of -24.7° aTDC. This work has demonstrated that combustion at a fixed f-EGAI can be maintained through advanced ignition control of CIM without experiencing heavy knocking events.

*Keywords:* Cooperative Fuel Research Engine, Auto Ignition, Exhaust Gas Recirculation, Response Surface Method

*Word Count:* 4988

## INTRODUCTION

Improvements in natural gas (NG) engine efficiencies while maintaining ultra-low NO<sub>x</sub> emission levels are necessary to realize future NG fuel demand goals and exploit the economic and environmental benefits of NG. Targeting higher efficiencies and NO<sub>x</sub> emission levels that will compete with future electrified fleet will require technological improvements in areas such as high CR, fast combustion, and advanced combustion phasing so that increased efficiency can be reached. However, the occurrence of end gas auto-ignition (EGAI) prevents using the optimal theoretical values for each of these parameters as an engine is typically designed with a knock margin or safety factor by reducing CR or retarding combustion phasing [1].

EGAI is characterized by low-temperature chemistry and self-heating of the gas ahead of the flame front due to the rising pressure and compressive temperature resulting from the propagating flame [2]. Often viewed as adiabatic compression conditions, this end-gas starts its own low-temperature chemical reactions. If left long enough under these conditions, radical build-up can occur in the end-gas and trigger rapid combustion of the fuel in this vicinity. Radical formation and EGAI are heightened in larger n-alkane hydrocarbon species due to unique low-temperature combustion kinetics, posing challenges to natural gas fuels that have high variability in these species' concentrations [3]. If the flame front is fast enough and the auto-ignition reactions slow enough, then the flame will consume the end gas prior to EGAI. Historical approaches have been to move toward rapid burn rates and slow auto-ignition reactions (e.g., running lean, diluting with EGR, or controlling fuel chemistry) [4].

Engine combustion strategies utilizing lean mixtures or exhaust gas recirculation (EGR) can lead to high cycle-to-cycle ignition variation [5]. Since only the most advanced combustion event might trigger the uncontrolled knock, the average cycles must be retarded to ensure the most aggressive cycle does not knock, translating into a net loss in efficiency. One of the key strategies proposed here is to move the most aggressive cycle closer to the average cycle by cycle resolved control thereby shrinking the knock margin and recovering efficiency benefits [6]. To do this requires an in-depth understanding of the knock/EGAI phenomenon, inherently stable combustion, and a control system that can maintain optimal combustion phasing while fuel, engine, and atmospheric conditions change. Such a system can minimize the knock margin under all conditions and enable maximum efficiency.

For stoichiometric combustion, operating at high compression ratios (CRs), closer to severe knock limited operational conditions, will achieve higher efficiencies and engine power. The decision to run stoichiometric was influenced by the benefit of reduced emission generations from the use of a three-way catalyst with stoichiometric exhaust [7]. Running at high CR will require the use of high concentrations of cooled EGR with advanced real-time controls to monitor and optimize EGR rates and combustion phasing. Increases in EGR, despite allowing for higher CR, slows burn rates (laminar flame speeds decrease 5-fold going from 0 - 30% EGR) [8] shifting a majority of heat release away from minimum volume and potentially preventing complete burn, negatively affecting fuel economy and resulting in unburned hydrocarbon emissions [8]. Furthermore, EGR dilution can increase the cycle to cycle variability and was utilized at levels that maximize CR while

achieving stable combustion [9]. Issues related to EGR dilution can be mitigated by increasing flame propagation by way of increased turbulent mixing while also enhancing flame initiation with advanced ignition technologies.

Two compelling reasons to use NG as a substitute for diesel fuel are to reduce particulate matter emissions and fuel costs. Currently in the U.S., the cost of diesel fuel on an equivalent energy basis is approximately five times the cost of NG [6]. NG engines, however, are typically less efficient than diesel engines, especially in the on-road medium and heavy-duty engine markets.

NG engines offer several advantages over diesel engines including lower particulate matter emissions, lower capital and operating costs, availability of vast domestic NG resources, and lower CO<sub>2</sub> emissions [3]. With the appropriate exhaust aftertreatment system both NG and diesel engines can meet ultra-low emission limits. However, the exhaust aftertreatment systems used for diesel engines are much more complex, requiring in many cases an oxidation catalyst, diesel particulate filter, and a selective catalytic reduction system [11]. Most current medium-duty NG engines use a single aftertreatment component, a 3-way catalyst, and therefore the aftertreatment system is less complex and lower cost. Market penetration of NG engines for mobile applications has been slow due to limited fueling infrastructure, lower engine efficiency, and lower power density [12]. The second two limitations are closely related since increasing engine power density, or brake mean effective pressure (BMEP), is a practical approach for increasing engine efficiency [13].

The objective of this study is to determine, describe, and analyze a practical method of controlled end gas auto-ignition (C-EGAI), and its effects on spark ignited, stoichiometric natural gas engine performance. The experiments were conducted on a cooperative fuel research (CFR) engine utilizing a premixed natural gas blend with a methane number of. The CFR engine was controlled with advanced ignition control through a Woodward Large Engine Control Module (LECM) to control the level of auto-ignition in the engine. High-speed pressure measurements and crank angle resolved cylinder pressure data characterized the combustion processes and quantify the magnitude of end gas auto-ignition (EGAI) event. Post processing software written in LabVIEW and the Woodward (LECM) enabled in-depth analysis of the required data sets.

## MATERIALS AND METHODS

### *Cooperative Fuel Research Engine*

The type of engine used in this project is a Cooperative Fuel Research (CFR) F-2 model Waukesha engine. It is a stationary, constant speed (~900 rpm), un-throttled, single cylinder, 4-stroke engine with a cylinder bore of 3.250 inches (8.255 cm) and piston stroke of 4.50 inches (11.43 cm). The displacement volume of the engine is 37.33 in<sup>3</sup> (611.7 cm<sup>3</sup>). To enable operation at a range of compression ratios from 4:1 to 18:1 the engine is constructed with a can-type casting forming the cylinder and cylinder head as a single part. The exterior of the cylinder is configured with a jack-screw type threaded race allowing an engaged worm-gear to raise and lower the cylinder relative to the piston/connecting rod assembly, held laterally stable in a clamping sleeve. By raising or lowering the cylinder the clearance volume (that volume formed from the top of the piston at TDC, the cylinder wall and the cylinder head) is

increased or decreased resulting in an adjustment of the compression ratio. The total vertical travel of the cylinder relative to the fixed position of the crankshaft is 1.235 inches. The engine allows adjustment of compression ratio while operating [14]. Figure 1 provides a cut-away drawing of the engine cylinder and clamping sleeve sections.

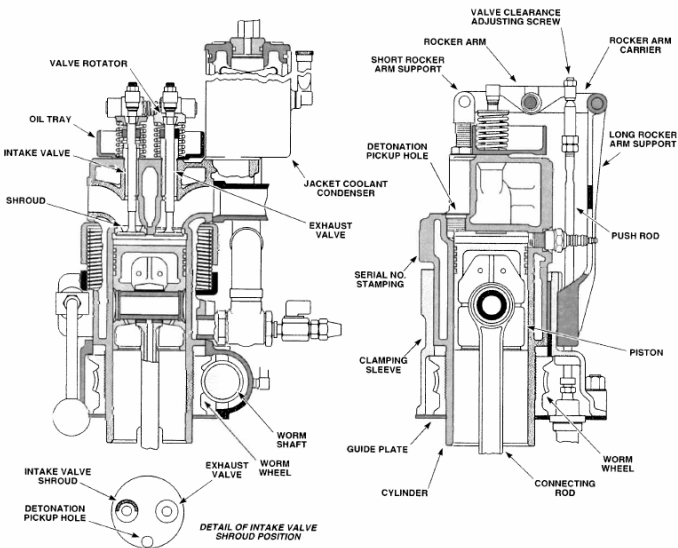


Figure 1: Cutaway of Original CFR Engine Cylinder Assembly [15].

The engine used in this project was manufactured in 1957 and is a model still manufactured and sold today, designed specifically for testing knock tendencies of fuels. Initially configured for octane number testing of gasoline blends, the engine is currently configured to burn gaseous fuels. There are numerous differences/modifications between the original Waukesha CFR engine and the CFR engine used in this testing. A Yaskawa regenerative Variable Frequency Drive (VFD) was installed for fine speed control at a range of speeds from 600 to 1200 RPM. High-speed Kistler piezo resistive intake (Type 4007D) and water-cooled exhaust (Type 4049B) pressure transducers were installed. Additionally, the engine conversion from liquid fuel to gaseous fuel created the requirement for an in-depth fuel blending system. The fuel blending system included the implementation of Omega differential flow meters of up to eight different flow constituents, as well as a Coriolis flow meter for total fuel flow. The final upgrade to the original CFR engine includes a Woodward Large Engine Control Module (LECM) engine control system. This system provided more accurate ignition control, and the ability to implement and test various ignition control schemes such as CA50 (control location of 50% mass fraction burned) and Combustion Intensity (Woodward defined metric of combustion control). Other modifications from the original engine configuration performed during previous work are described in references [14] [15]. Table 1 outlines the initial operating conditions throughout the testing.

Table 1: Operating Conditions of the CFR engine

Fuel MN	71
Lambda	1 ± 0.01
Intake Pressure	150 kPa
Intake Temperature	65 °C
Coolant Temperature	95.5 °C
Oil Temperature	130 °F
Exhaust Temperature	535 °C
CR	10:01
Engine Speed	900 RPM
IMEP	1000 kPa
Electric Output Power	2.5 kW
Ignition Timing	15° bTDC
CA50	8° aTDC
COV PP	5.4

### Exhaust Gas Recirculation Test Cart

A crucial piece of equipment required for the testing performed for this study, was the Exhaust Gas Recirculation (EGR) test cart that was fabricated for use with the CFR engine. The cart design was inspired by one previously fabricated for engine testing at Woodward Inc. EGR is commonly used for increasing power density, reducing NOx emission concentrations, and causing knock suppression for operation at higher power densities. The CFR engine does not include EGR systems with the base unit, and thus a cart that can replicate the functions of a high-pressure EGR loop while providing a wide range of possible flows was necessary.

For this project, the EGR cart was required to be able to provide the CFR engine with a maximum EGR rate of 40% at maximum load. Utilizing previously supplied engine data from the CFR engine, flow rates were extrapolated to expect ~ 115 grams per minute of exhaust gas at a max load of 3.5 kW. Initial testing after the fabrication of the EGR cart showed that the maximum optimal EGR rate was only 74 grams per minute at 3.5 kW of electric power output. However, this was more than adequate for the present study. The final EGR cart is shown below in Figure 2.



Figure 2: Custom Exhaust Gas Recirculation Test Cart for CFR Engine.

### Knock Measurement and Quantification

The knock measurement system for the CFR engine begins with a water-cooled, piezoelectric transducer (Kistler model 6061A) mounted in the same cylinder detonation port previously housing the Type D-1 pickup. The signal from the transducer feeds to a charge amplifier which relays pressure signal input to the controlling software. A rotary 0.1° incremental optical engine encoder (BEI model L25) provides positive crank angle position indication enabling real-time display of cylinder pressures as a function of crank rotation.

The LECM provides a single-box approach that can be built up with interlocking modules into a single engine-mountable assembly [16]. Each module within the LECM has a microprocessor and runs software routines, written in Woodward's MotoHawk® software, using proven core functions and algorithms. The main module software can also be written in Woodward's Graphical Application Programmer (GAP™) [17]. The modules all share their information in a real-time manner, making the entire system act as one fully integrated control.

Utilizing the same cylinder pressure acquisition system and equipment as the LabVIEW control scheme, the LECM is capable of live data processing. This includes heat release rates, knock intensity, advanced combustion analysis, CA50, combustion intensity, IMEP, NMEP, PMEP, and historical pressure traces, each of which are updated every 1 seconds (~13 cycles) [17]. The LECM does not monitor pressures, temperatures, flow rates, power outputs, or EGR rate for the CFR engine because it is primarily controlled through the LabVIEW control scheme, leaving the LECM's primary function to be cylinder pressure analysis.

The quantification of engine knock is what allows for the realization of C-EGAI, providing the ability to determine the fractional heat release due to auto-ignition (f-EGAI). The f-EGAI is the percent of energy available in the cylinder after auto ignition begins [18]. In this study, it was assumed that the f-EGAI is equal to the full amount of remaining heat release. Controlling the f-EGAI to a predetermined level will hold the engine in a steady state beyond the traditional knock limit, thus improving combustion efficiency, reducing combustion durations, improving power output, and increasing total system efficiency. F-EGAI is the best metric to compare the level of auto-ignition that occurs within the cycle to additional cycles no matter the running conditions, and thus is the correlation to C-EGAI.

The f-EGAI to C-EGAI correlation is rooted in the knock onset crank angle (KOCA). This is determined with the calculation of the third derivative of the cylinder pressure trace [19]. By taking the third derivative, the inflection point that signifies the start of the secondary ignition event (auto-ignition) within the cycle is isolated as the x-intercept of the third derivative plot. This inflection point demonstrates the increased rate of pressure rise and the exact crank angle upon which it begins, which is determined to be the KOCA. By applying the KOCA value to the mass fraction burned plot for the cycle the F-EGAI can be determined by the remaining mass fraction within the cylinder following the KOCA. Figure 3 demonstrates the third derivative KOCA calculation for a heavy knocking case.

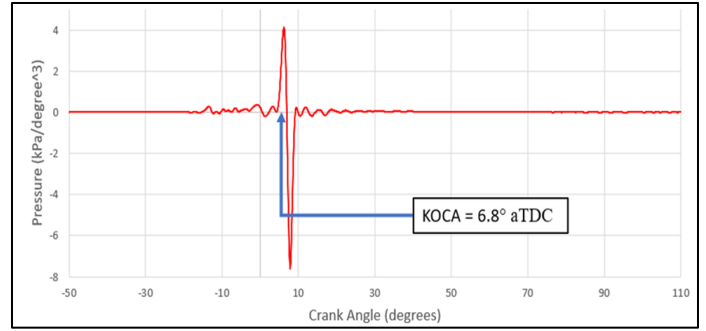


**Figure 3: Third Derivative of the Cylinder Pressure Trace for Determining KOCA values – Represented on a Heavy Knocking Case.**

Five different methods were found within the literature [20][21][22][23] and evaluated for their knock quantification abilities utilizing previously collected CFR engine data. These methods are briefly outlined in Table 1. The knock intensity quantification methods that were analyzed include: Fast Fourier Transform, knock ripple sum, peak rate of pressure rise (1st derivative), the maximum amplitude of the bandpass filtered cylinder pressure, and the integral of the bandpass filtered cylinder pressure. Each method was evaluated for its ability to detect the occurrence engine knock, locate the knock onset crank angle, differentiate between the various level of engine knock, and correlate linearly with f-EGAI.

The FFT and Knock Ripple Sum methods were the primary methods utilized for verification of C-EGAI during operation of the CFR engine. Auto ignition events were quantified during live operation and the parameters of the CFR were adjusted to aid in C-EGAI implementation.

**Table 2: Knock Quantification Techniques Considered for Use as C-EGAI Control Scheme.**

METHOD	SOURCE	DESCRIPTION
FFT OF BANDPASS FILTERED SIGNAL	Colorado State University	Time averaged analysis of frequencies in knock signal pressure trace
MAXIMUM AMPLITUDE OF BANDPASS FILTERED SIGNAL	Cummins LLC	Knock intensity related to maximum frequency in pressure signal
INTEGRAL OF BANDPASS FILTERED SIGNAL	B. Radu et al. University POLITEHNICA of Bucharest	Knock intensity related to maximum positive value of integral
RATE OF CYLINDER PRESSURE CHANGE	B. Radu et al. University POLITEHNICA of Bucharest	Highest value of pressure trace after first crank angle resolved derivative
THIRD DERIVATIVE OF CYLINDER PRESSURE TRACE	J. Amador Diaz, et al. Universidad del Norte	Rise in amplitude of third derivative correlated to knock onset crank angle
KNOCK RIPPLE SUM	Woodward Inc.	Subtract a running average pressure trace from current knocking trace

### Combustion Intensity

Through the evaluation of the different knock quantification techniques, the most promising method is to utilize ignition timing control, due to its high correlation with knock severity. The LECM ignition system was utilized to control a parameter programmed into the LECM called “Combustion Intensity” [16][17]. This method utilizes multiple operational engine parameters and takes a weighted average of each to determine where on a 0 to 100% scale the engine is operating. The results from previously evaluated methods of knock quantification were considered with this method of ignition control.

Equation 1 shows the weighted average to calculate combustion intensity with the given conditions of the engine where:

**P<sub>max</sub>** = Peak Cylinder Pressure  
**BD** = Burn Duration  
**PRR** = Peak Rate of Pressure Rise  
**HRRs** = Heat Release Rise Rate Slope  
**KI** = Knock Intensity (Knock Ripple Sum Method)  
**A1 through A5** = Calibration Constants

$$\begin{aligned}
 CIM = A_1 \left( \frac{P_{max}}{P_{max_{ref}}} \right) + A_2 \left( \frac{BD}{BD_{ref}} \right) + \\
 A_3 \left( \frac{PRR}{PRR_{ref}} \right) + A_4 \left( \frac{HRRs}{HRRs_{ref}} \right) + A_5 \left( \frac{KI}{KI_{ref}} \right) \quad \text{Equation 1}
 \end{aligned}$$

By dividing the recorded value of the five variables by their engine operational defined maximums, the variables are normalized to a unitless percentage of full scale for comparison to different engine platforms. By standardizing knock intensity alongside the other four parameters inside the combustion intensity metric, the operational condition of the engine is more comparable across all loads.

To implement C-EGAI using CIM as the control parameter, a correlation between CIM and f-EGAI was investigated. A valid justification for the use of combustion intensity as the control parameter for C-EGAI was discovered within this study.

#### Response Surface Method

To determine the effectiveness of C-EGAI on a stoichiometric, spark-ignited, natural gas engine, a system optimization was performed. The efficiency optimization method selected was a type of Response Surface Method (RSM) that was determined suitable for this application. This method is deemed the Modified Box-Benken Design [24][25]. Figure 4 displays a graphic to help explain the RSM. To properly map the operational conditions of an engine, a multidimensional space of N dimensions, where N = number of variables to be optimized, is created and every data point within that space is evaluated to generate a complete surface map of performance. The modified Box-Benken design allows the operator to take a select origin point within the N-dimensional space and test every point around the origin in predetermined step sizes and generate a vector equal to the merit function defined by the RSM. The vector is then followed until the merit function reaches a maximum value, and the process of generating the vector around the new maximum is repeated until the new vector's travel is within the known noise of the system. In this case there are five variables, so thus a 5-dimensional space. The merit function is equal to the brake efficiency of the CFR engine.

The five variables that were varied within this optimization were: Indicated Mean Effective Pressure (IMEP), Engine Speed, EGR Rate, Compression Ratio, and Combustion Intensity. The

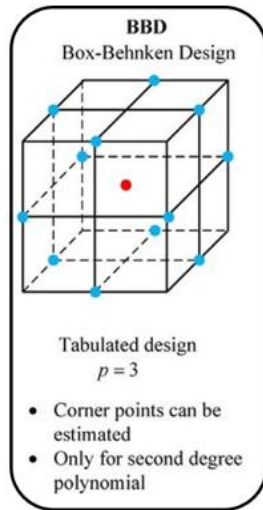


Figure 4: Modified Box Behnken Design Response Surface Method [24].

efficiency optimization will validate the location of these peak efficiency values and determine the optimal conditions for the CFR engine under stoichiometric, spark ignited, natural gas conditions with EGR and C-EGAI.

## RESULTS

Cylinder pressure traces for baseline data were collected. These data sets hold the CFR engine at performance point like the methane number research method parameters, with a “stock” data point as well as the inclusion of EGR and points operating near and at the knock limit of the CFR engine. The knock limit is represented as the onset of noticeable auto-ignition events through the FFT Power Spectrum method of knock quantification [21]. The data is represented in Figure 5 through an average of 1000 cycles. This will be the comparison point for available efficiency gains in future data sets.

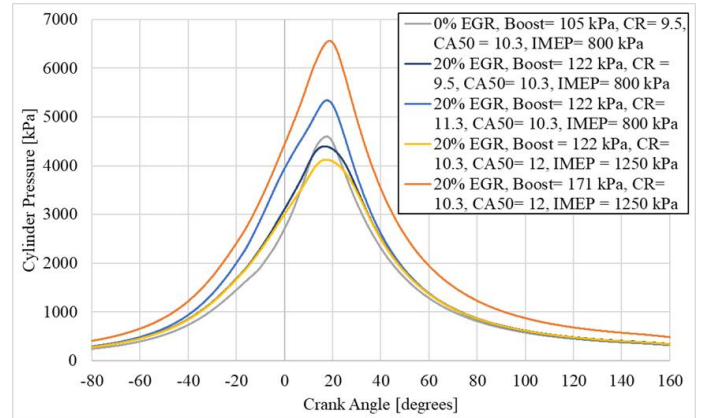


Figure 5: Baseline CFR Engine Data with EGR and Knock Limit cases.

A previous study on the CFR engine examined the EGR limits of a stoichiometric, spark-ignited, natural gas CFR engine under these conditions, and found a viable brake efficiency gain of 2.8 efficiency points through operating at the maximum EGR limit of 21% EGR replacement of the intake air/fuel mixture.

To implement C-EGAI, a control scheme was created through the CIM explained prior. To fully analyze the effect of CIM on the CFR engine under the given conditions, a sweep of the usable CIM domain was conducted and is shown in Figure 6 for a 15% EGR case. The CIM value was unable to exceed 80% due to the knock intensity reaching the absolute knock limit of the engine, at an FFT knock intensity value of 3000 kPa rms<sup>2</sup>.

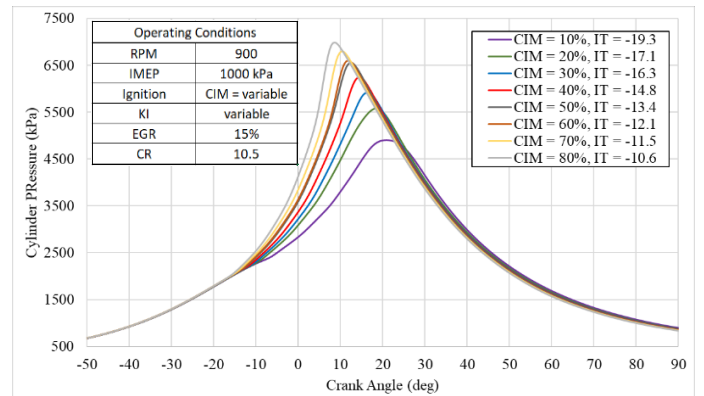


Figure 6: 10% to 80% CIM Sweep on CFR Engine at Given Conditions.

Figures 7 and 8 show the efficiency and combustion stability through coefficient of variation (COV) of peak pressure (PP) for the 0% EGR case as well as an additional sweep of CIM with 15% EGR. These figures lead one to believe that the inclusion of CIM control on the CFR engine under the given conditions can provide viable brake efficiency gains while maintaining proper combustion control.

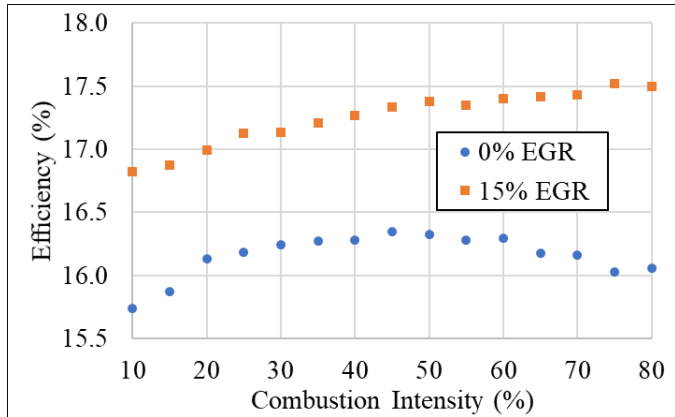


Figure 7: Brake Efficiency Values from 10% to 80% CIM Sweeps on CFR Engine.

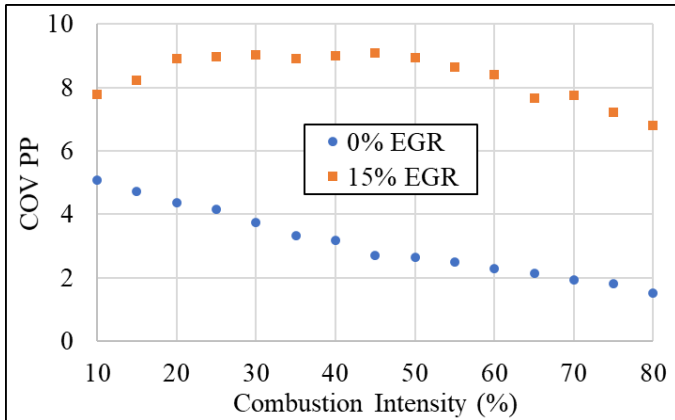


Figure 8: Coefficient of Variance of Peak Pressure for Combustion Stability Analysis on CFR Engine for 10% to 80% CIM Sweep on CFR Engine

As described, CIM is a metric of ignition timing control, and through Figure 6 it is seen that ignition timing is advanced with the increase of CIM. Additionally, the five variables of CIM are proving to increase as CIM increases with Figures 6 and 9, with the most dominant effect being the onset of auto-ignition events for all data points after a CIM of 30%. The AHHR analysis in Figure 9 also proves the increased combustion stability at each level of CIM along with the linear increase in combustion intensity.

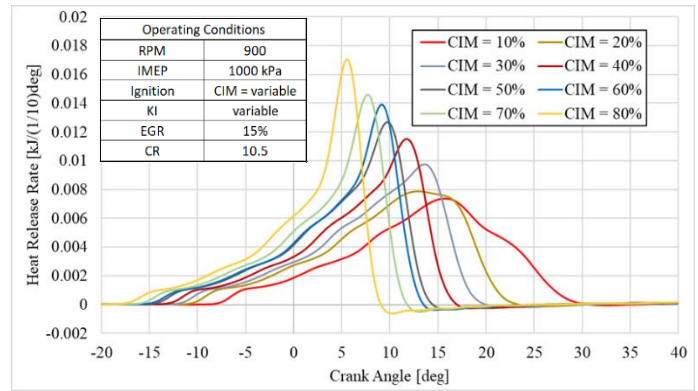


Figure 9: AHHR for 10% to 80% CIM Sweep on CFR Engine at Given Conditions.

To further verify that CIM is a viable metric of implementing C-EGAI, a trend had to be defined between the two metrics. The closest relative parameter to C-EGAI is f-EGAI, and through the third derivative method of calculating KOCA this trend was defined. The KOCA values for all the data points in the CIM sweep from Figure 6 were calculated and then used to correlate the f-EGAI. The KOCA and f-EGAI values for the full CIM sweep data set are shown in Figures 10 and 11. Figure 12 demonstrates relative efficiency values between data points of a CIM sweep for both the 0% and 15% EGR cases on the CFR engine.

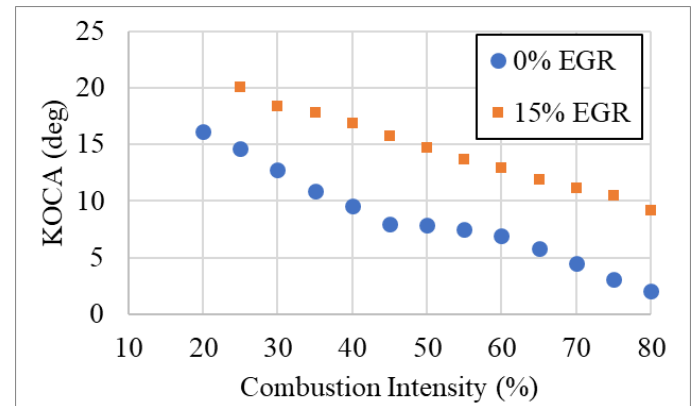


Figure 10: KOCA Values from 0% to 80% CIM Sweep on CFR Engine.

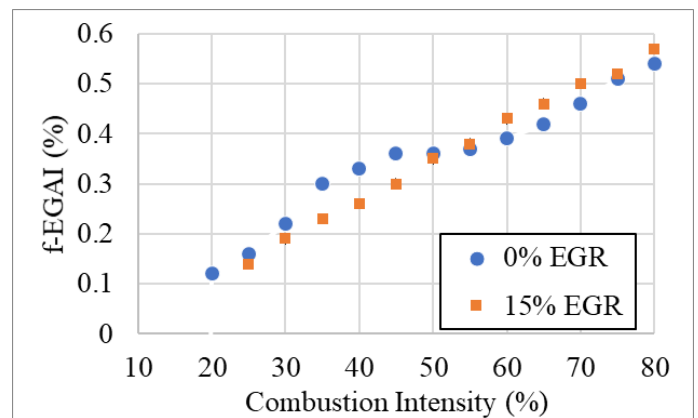


Figure 11: f-EGAI Values for 0% to 80% CIM Sweep on CFR Engine.

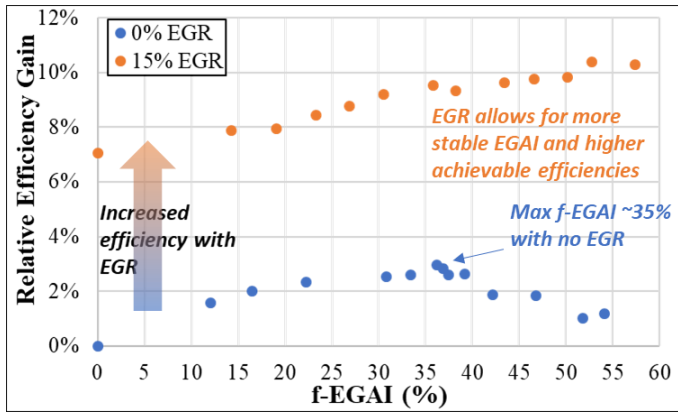


Figure 12: Relative Efficiency Values vs f-EGAI for 0% and 15% EGR Data Sweeps of CIM

There was no KOCA value detected for combustion intensities below 20% CIM without EGR and below 25% CIM with EGR. The lack of auto-ignition is likely because the combustion intensity was too low to instigate auto-ignition events at the given conditions of the CFR engine.

To transition into the efficiency optimization with C-EGAI, the five variables of optimization were individually swept across here operational ranges. These data sweeps are represented in Figure 13, where an intuitive investigation into the direction of steepest ascent from the initial operating point is provided.

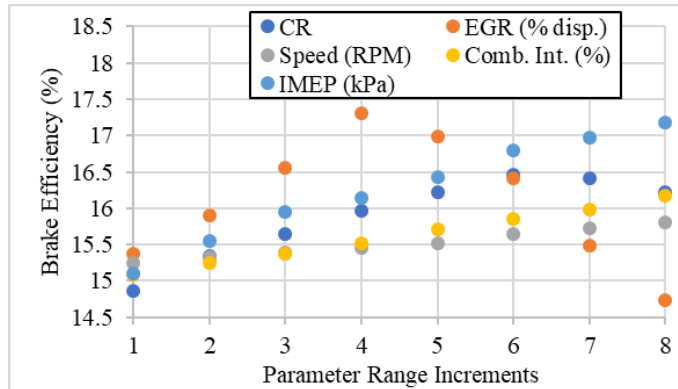


Figure 13: Brake Efficiency Trends for Five Variables of Efficiency Optimization.

Table 2 lays out the starting data point for the optimization taken from standard research method methane number testing, as well as the final data point of peak efficiency. These values were used with the merit function of brake efficiency to generate the vectors of merit function improvement. The total RSM efficiency optimization took four stages of vectors to reach peak performance. Table 4 lays out the center points and step sizes used to generate the vectors for each stage within the sphere of influence, and the operational limits that the merit function could not exceed.

Table 3: Starting and Final Data Points of RSM Efficiency Optimization.

	Starting Data Point	Final Data Point
IMEP (kPa)	1000	1150
Speed (RPM)	900	1080
EGR (% Disp.)	12	17.8
CR	10	10.55
CIM (%)	30	39.5

Table 4: Vector Stage Centers, Step Sizes, and Operational Limits of the Five Optimized Variables on the CFR Engine

Stage 1					
	Speed	EGR	CR	IMEP	CIM
center	900	12	10	1000	30
+1	950	15	10.5	1050	35
-1	850	9	9.5	950	25
Stage 2					
	Speed	EGR	CR	IMEP	CIM
center	1150	15.4	10.3	1100	35.5
+1	1200	18.4	10.8	1150	40.5
-1	1100	12.4	9.8	1050	30.5
Stage 3					
	Speed	EGR	CR	IMEP	Comb. Int.
center	1100	16.8	10.6	1150	37.5
+1	1150	19.8	11.1	1150	42.5
-1	1050	13.8	10.1	1150	32.5
Stage 4					
	Speed	EGR	CR	IMEP	CIM
center	1080	17.5	10.55	1150	39.5
+1	1130	20.5	11.05	1150	44.5
-1	1030	14.5	10.05	1150	34.5
Operational Limits					
	Speed	EGR	CR	IMEP	CIM
	1200	30	18	1300	80

Figure 14 shows the cylinder pressure traces from the four stages of efficiency optimization. The four different stages are defined by the four different set of vectors resulting from the Modified Box Behnken Design Response Surface Method. Each set of vectors is generated from a pre-determined center point, and marches along a designated step size until a relative maximum value of the merit function is reached. The last set of vectors identifies the true maximum value of the merit function when the vectors cause the merit function to no longer increase in value. It can be seen that immediately after the first stage, the CFR engine was taken into the knock window, evident through the secondary pressure rise, while the increased operating speed, increased IMEP, increased EGR, and advanced ignition timing through increased CIM are evident by the stretched and taller pressure traces of later stages. It can also be seen that the first stage caused a large movement of the CFR engine, while the additional stages were the fine adjustments of the five variables.

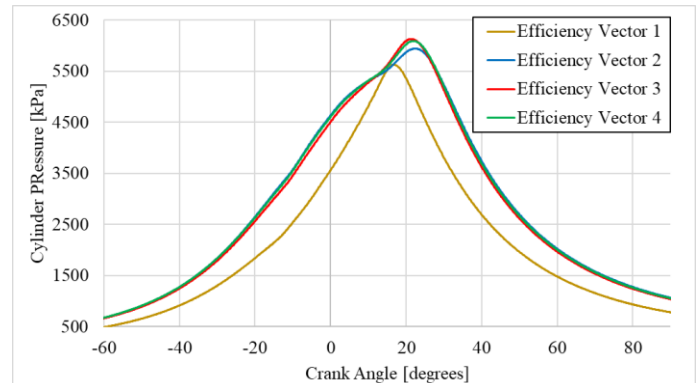


Figure 14: Cylinder Pressure Traces from the Four Stages of Efficiency Optimization Vectors.

The brake efficiency values from each stage of the optimization within the four vectors is shown in Figure 15. The figure shows a brake efficiency improvement from 17.7% to 21.3%. This is a 3.6 efficiency point gain within the optimization, as well as a 1.2 efficiency improvement over the previous greatest brake efficiency found through EGR implementation under these given conditions [26].

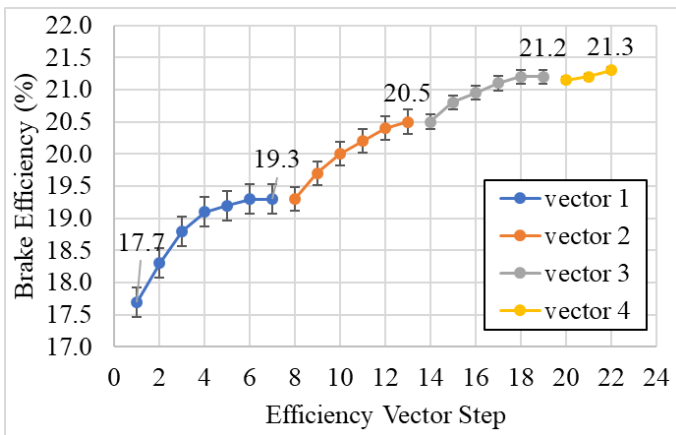


Figure 15: Brake Efficiency Values from Each Stage of RSM Efficiency Optimization.

The f-EGAI levels are shown from the optimization in Figure 16. The point of peak performance demonstrated a 34.1% f-EGAI, which correlates directly to C-EGAI. This says that controlling the CFR engine to a 34.1% level of C-EGAI with the other prescribed conditions will inhibit the point of peak performance on the CFR engine.

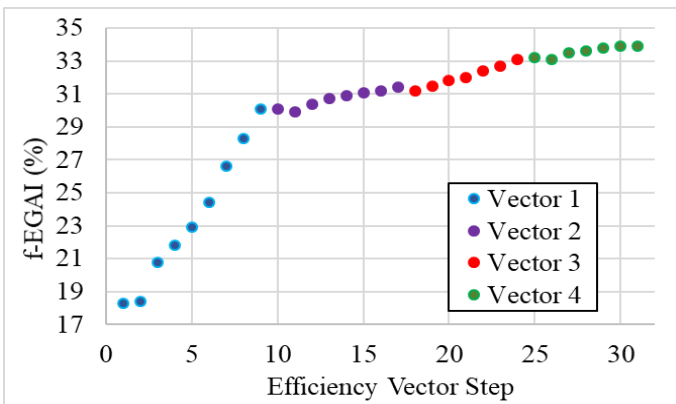


Figure 16: f-EGAI values from Each Stage of RSM Efficiency Optimization for C-EGAI correlation on CFR Engine.

## DISCUSSION

The implementation of C-EGAI on a stoichiometric, spark-ignited, natural gas engine exhibited beneficial improvements to the system in various methods. First is the increase in combustion efficiency through end gas auto-ignition consuming the end gas that is often burned late in the cycle. Additionally, controlling the level of auto-ignition through ignition control minimizes the negative effects of auto-ignition events by preventing the knocking cycles from escalating during subsequent cycles. This reduces the chance of percussive force damage nor corrosive damage through high temperature combustion exposure to the cylinder walls from reducing the operating life of the engine. The brake efficiency of the CFR

engine saw a 3.6 efficiency point gain over the optimization of the primary engine parameters.

Through attempting to control the auto-ignition events for every cycle of the engine, the overall combustion event was stabilized better than any prior attempts by using CIM. By using the five variables outlined in CIM, it considers various parameters of the engine outside of auto-ignition. Thus, the load, speed, ignition timing, and boost pressure are considered, and the CIM percentage is adjusted to maintain a stable level of the combined effects of the five variables.

C-EGAI was theorized to be most effective at low to medium levels of auto-ignition. After the efficiency optimization, it was determined that the maximum efficiency occurred at 34.1% f-EGAI. Any C-EGAI level greater than 35% on the CFR engine created unstable combustion events that negatively impacted efficiency. At the 34.1% level of C-EGAI, the knock intensity through the knock ripple sum method of knock quantification determined a 38.3% knock intensity based on the 0% to 100% full scale range. This signifies a light to medium knock intensity, and correlates to moderate knock sinusoids with approximately one third of the heat release being due to auto ignition. The CFR engine cylinder is designed with a side mounted spark plug, so the f-EGAI level is most likely larger on the CFR engine at the given levels of CIM and C-EGAI than with a top mounted spark plug engine.

The most direct path to C-EGAI would be to control f-EGAI directly. However, the data presented in Figure 11 demonstrate a linear relationship between f-EGAI and CIM, the parameter pre-programmed into the LECM. It can be concluded that if CIM is effectively controlled the f-EGAI is effectively controlled.

The largest benefit of C-EGAI is the 20.3% relative efficiency gain (3.6 efficiency point gain) over the RSM efficiency optimization to a final brake efficiency of 21.3%. This is the highest recorded brake efficiency on this CFR engine by 1.2% compared to previous approaches applying a knock margin. Even at peak performance, the power density of the CFR engine is lower than most commercial engine platforms. The IMEP at peak performance was 1150 kPa with a 186 kPa inlet boost pressure. This operated beyond the previously prescribed knock limit of the CFR engine, allowing stable combustion with a steady location of peak pressure and CA50 with COV levels below 6.5%.

Moving forward with this study, the work will focus on implementing C-EGAI on different engine platforms starting with a 15 L, 6 cylinder, Cummins X15 engine converted to a single cylinder research engine under the same natural gas conditions. This will determine if the factors of C-EGAI are the same across multiple engine platforms. Additional future work involves exploring the effect of C-EGAI on a transient load engine, since the CFR engine was tested only with static data points of engine load and speed. On a similar note, it would be beneficial to explore additional combustion control and knock quantification strategies to see if CIM could be improved upon for future C-EGAI implementation.

## CONCLUSION

In conclusion, this work is the first to report the application of controlled end gas auto-ignition in a stoichiometric, spark ignited, natural gas engine. The results show distinct advancements towards increased brake efficiency on a CFR engine through C-EGAI and RSM optimization of multiple

engine variable. It is demonstrated that CIM is positively related to f-EGAI with a clear linear regression and, thus, CIM control is an adequate control scheme for C-EGAI. At maximum efficiency operating condition, the CFR engine exhibits a brake efficiency of 21.3%, at a f-EGAI level of 34.1%. Given these encouraging results, it is important that the same approach be explored on industrial engine platforms to better quantify potential benefits.

## ACKNOWLEDGMENTS

This work was funded by the Department of Energy through the Office of Energy Efficiency and Renewable Energy. The authors would like to thank our project partners, Cummins Inc. and Woodward Inc. for their valuable contributions.

## REFERENCES

[1] Brunt, M. Pond, C. Biundo, J. "Gasoline Engine Knock Analysis Using Cylinder Pressure Data." SAE International. 980896. 1998 pp. 118.

[2] Elmqvist, C. et al., 2003. Optimizing Engine Concepts by Using a Simple Model for Knock Prediction, s.l.: SAE International.

[3] Elgohary, Mohamed. Seddiek, Ibrahim. Salem, Ahmed. "Overview of Alternative Fuels with Emphasis on the Potential of Liquefied Natural Gas as Future Marine Fuel." Institute of Mechanical Engineers. Sage journals. 2014.

[4] Hockett, Andrew. Hampson, Greg. Marchese, Anthony. "Sensitivity Study on Natural Gas/Diesel RCCI CFD Simulations Using Multi-Component Fuel Surrogates." Int. J. Powertrains. 2016.

[5] Szybist, James P., et al. "The Reduced Effectiveness of EGR to Mitigate Knock at High Loads in Boosted SI Engines." SAE International Journal of Engines, vol. 10, no. 5, 2017, pp. 2305–2318. JSTOR.

[6] Li, Hailong. Haugen, Geir. Ditaranto, Mario. Berstad, David. And Jordal, Kristin. "Impacts of Exhaust Gas Recirculation (EGR) on the Natural Gas Combined Cycle Integrated with chemical Absorption CO<sub>2</sub> Capture Technology." Energy Procedia. Vol. 4, 2011, pp. 1411 – 1418. 24

[7] Pulkrabek, W. W., 2004. Engineering Fundamentals of the Internal Combustion Engine. 2nd ed. Upper Saddle River (New Jersey): Pearson Prentice Hall.

[8] Hoepke, Bjoern, et al. "EGR Effects on Boosted SI Engine Operation and Knock Integral Correlation." SAE International Journal of Engines, vol. 5, no. 2, 2012, pp. 547–559. JSTOR.

[9] Tutak, Wojciech. "Numerical Analysis of the Impact of EGR on the Knock Limit in SI Test Engine." Institute of Internal Combustion Engines. Vol. 21. 2011. Pp 397-406.

[10] Amann, Manfred, et al. "The Effect of EGR on Low-Speed Pre-Ignition in Boosted SI Engines." SAE International Journal of Engines, vol. 4, no. 1, 2011, pp. 235–245. JSTOR.

[11] Grondin, Oskar. Moulin, Peter. Chauvin, James, "Control of a turbocharged Diesel engine fitted with high pressure and low-pressure exhaust gas recirculation systems." Proceedings of the 48th IEEE Conference on Decision and Control (CDC) held jointly with 2009 28th Chinese Control Conference, Shanghai, 2009, pp. 6582-6589.

[12] Amador Diaz, German. Gomez Montoya, Juan. Corredor Martinez, Lesme. Olsen, Daniel. Salazar Navarrows, Adalberto. "Influence of Engine Operating Conditions on Combustion Parameters in a Spark Ignited Internal Combustion Engine Fueled with Fuel Blends of Methane and Hydrogen." Elsevier

Editorial System for Energy Conversion and Management. Manuscript. 2016.

[13] Fischer, M. Günther, M. Berger, C. Troeger, R. Pasternak, M. Mauss, F. "Suppressing Knocking by Using Clean EGR – Better Fuel Economy and Lower Raw Emissions Simultaneously." Knocking in Gasoline Engines. KNOCKING 2017. Springer, Cham. Pp. 363-384.

[14] Wise, Daniel. Olsen, Daniel. Caille, Gary. "Investigation into Producer Gas Utilization in High Performance Natural Gas Engines." Colorado State University, Mechanical Engineering; Dissertation. 2013.

[15] Waukesha Engine Division, Dresser Industries, 1980. The Waukesha CFR Fuel Research Engine. Waukesha(Wisconsin): Waukesha.

[16] Chiera, Domenico. Carlson, Jeff. Nair, Suraj. McCreery, Sam. Hampson, Gregory. "High Efficiency Natural Gas Engine Combustion Using Controlled Auto-Ignition." ASMA Internal Combustion Technical Conference. 2019.

[17] Nair, Suraj. Hampson, Gregory. Carlson, Jeffrey. "Controlled Multi-staged Combustion Strategy for Overcoming Load Limitations of Fuel Flexible Gas / Diesel Engines." New Engine Developments – Gas & Dual Fuel. CIMAC Congress. 2019.

[18] Brunt, M. Pond, C. Biundo, J. "Gasoline Engine Knock Analysis Using Cylinder Pressure Data." SAE International. 980896. 1998 pp. 118.

[19] Schmillen, Karl. Rechs, Manfred. "Different Methods of Knock Detection and Knock control." SAE International. vol. 225. 1991. Pp. 242-246.

[20] Burgdorf, Klaas. Denbratt, Ingemar. "Comparison of Cylinder Pressure Based Knock Detection Methods." SAE: Combustion and Emission Formation in SI Engines. 1997.

[21] Schmillen, Karl. Rechs, Manfred. "Different Methods of Knock Detection and Knock Control." SAE: Sensors and Actuators. 1991.

[22] Barton, R. Lestz, S. Duke, L. "Knock Intensity as a Function of Engine Rate of Pressure Change." Society of Automotive Engineers. 1970

[23] Xu, Hui. "CMI Knock Index Determination Method." Cummins Inc. 2018.

[24] Lian, Binbin. Sun, Tao. Song, Yimin. "Parameter Sensitivity Analysis of a 5-Dof Parallel Manipulator." Tianjin University: China. Robotics and Computer-Integrated Manufacturing. 46. 2017.

[25] NIST, SEMATECH. "Engineering Handbook of Statistical Methods." US Department of Commerce. 2013.

[26] Bayliff, Scott. Olsen, Daniel. Et. al. "The Effect of EGR on Knock Suppression, Efficiency, and Emissions in a Stoichiometric, Spark Ignited, Natural Gas Engine." Western States Section of the Combustion Institute Fall 2019 Technical Conference. Colorado State University. 2019.